CHAPTER 25

NUMERICAL SIMULTION OF INELASTIC, FRICTIONAL PARTICLE-PARTICLE INTERACTIONS

O. R. Walton

25.1 INTRODUCTION

Understanding the flow behavior of particulate suspensions as well as pneumatic and dry granular flows is important for such diverse applications as in-plant and long-distance transport, manufacturing of ceramics, casting of solid-fuel rocket propellant, preparation of pharmaceuticals and a wide variety of manufacturing, food, chemical and mineral processing operations. Current lack of understanding makes scaling from laboratory bench-top prototype operations to large-scale commercial plants more of a "cut-and-try" art, than a rational design process. New approaches that specifically take into account the micro structural nature of these materials have the potential to provide us with the ability to predict their flow behavior.

The focus of this volume is suspensions and multiphase flows, emphasizing how suspended solid particles affect the hydrodynamic stresses in the fluid. In many situations, however, direct contacts between the particles themselves strongly affect the stresses in the fluid-solid mixture and the interactions with boundaries. Hydrodynamic *lubrication* forces theoretically will prevent smooth spheres in suspension from coming in physical contact with each other, since such forces diverge as surfaces approach each other. However, depending on the surface roughness and the inertia of the particles, the density and viscosity of the fluid media, and on the deformation rate, actual physical contact between real particles is not only possible, but may be highly likely during dynamic flow conditions. In gas fluidized systems most particles exceeding a few microns in diameter are likely to experience particle-particle or particle-surface contacts. Similarly, in aqueous (or other similar liquid-) solid systems, particles exceeding a few 10's of microns in diameter are likely to experience some particle-particle contacts if the deformation rate is significant. Real particles come into contact with each other because their surface roughness exceeds the theoretical gap width that would produce a large enough hydrodynamic lubrication force to prevent such a contact. Leighton (1992) discusses this point further in Chapter 6 of this volume. At high deformation rates particle-particle collisions may even dominate the behavior of many multiphase systems. Bagnold (1954) termed the regime of flows where particle collisions dominate the behavior the *grain-initeria*

regime. Ahn and Brennen (1992) discuss Bagnold's criteria in Chapter 7 of this volume. After a brief review of methods used to calculate the behavior of fluid-solid systems this chapter discusses in detail various numerical and theoretical models of particle-particle interactions and the resulting behavior of assemblies of particles undergoing such interactions. Subsequent chapters (*i.e.*, Brady, 1992; Kim and Fuentes, 1992; Prosperetti and Sangami, 1992) discuss various approaches being taken to numerically simulate the behavior of suspensions, specifically including the hydrodynamic interactions carried by the interstitial fluid.

25.1.1 Stress Tensor in Fluids

The momentum flux density tensor in an *ideal* fluid is given by

$$\bar{\Pi} = p\,\bar{\mathbf{I}} + \rho\mathbf{uu} \tag{25.1}$$

where $\rho\mathbf{u}$ is the momentum of a unit volume and p is the equilibrium pressure. The term $\rho\mathbf{uu}$ represents the momentum flux due to the bulk motion of the fluid. For a *viscous* fluid a term, $-\bar{\mathbf{T}}'$, which gives the irreversible "viscous" transfer of momentum in the fluid (from regions of high momentum to regions of low momentum), must be added to the total momentum flux density. The stress tensor, $\bar{\mathbf{T}}$, which is that part of the momentum flux tensor that is not due to the bulk fluid motion (*i.e.*, the negative of the pressure tensor) then is given by (Landau and Lifshitz, 1959)

$$\bar{\mathbf{T}} = -p\,\bar{\mathbf{I}} + \bar{\mathbf{T}}' \,. \tag{25.2}$$

For a Newtonian fluid the stress tensor has the form (Hoover, 1991)

$$\bar{\mathbf{T}} = (-p + \lambda\,\nabla\cdot\mathbf{u})\bar{\mathbf{I}} + \eta(\nabla\mathbf{u} + \nabla\mathbf{u}^t) \tag{25.3}$$

where the equilibrium pressure p and the two viscosity coefficients η and λ all depend on the local thermodynamic state, and the superscript t indicates the transpose of the velocity gradient tensor $\nabla\mathbf{u}$. The "bulk" viscosity, which gives the excess pressure in compression and excess tension in expansion is

$$\eta_v = \lambda + (2/3)\eta \,. \tag{25.4}$$

If the fluid flow is incompressible, then $\nabla\cdot\mathbf{u} = 0$, so the bulk viscosity does not influence the flow, and the stress tensor simplifies to

$$\bar{\mathbf{T}} = -p\,\bar{\mathbf{I}} + \eta(\nabla\mathbf{u} + \nabla\mathbf{u}^t). \tag{25.5}$$

25.1.2 Stress Tensor in Particulate Systems

For a system of particles with no interstitial fluid, interacting via pairwise additive forces $\mathbf{f}_{ij}$, the instantaneous stress tensor averaged over the volume V, is given by (Evans, 1979; Irving and Kirkwood, 1950)

$$\bar{\mathbf{T}}_p = \frac{1}{V}\sum_i m_i(\mathbf{v}_i - \mathbf{u}_i)(\mathbf{v}_i - \mathbf{u}_i) + \frac{1}{V}\sum_{i>j}\mathbf{f}_{ij}\,\mathbf{r}_{ij} \tag{25.6}$$

where the first term represents the momentum carried by the particles themselves in their fluctuations about the mean velocity field $\mathbf{u}$. This term is often called the *kinetic* contribution to the stress. The subscript i on $\mathbf{u}$ indicates the value of the mean field at the instantaneous location of the ith particle. The velocity and mass of the ith particle are given by $\mathbf{v}_i$ and m_i, respectively. The second term, called the *potential* contribution, represents

the rate of momentum transfer from one particle to another due to the interaction force $\mathbf{f}_{ij}$, where $\mathbf{r}_{ij}$ is a vector from the centroid of the ith particle to the centroid of the jth particle. The sum is over all interacting near neighbors. The first term is symmetric but the second term can include non-symmetric components if the interaction force is not central (Evans, 1979). If the interactions between particles are approximated by instantaneous collisions, then the last term is replaced by an average of momentum transfers due to collisions between particles (Chapman and Cowling, 1952).

25.1.3 Approximate Stress Tensor in Suspensions

In suspensions the stress distribution around each suspended particle is influenced by all other particles in the system. The stress tensor, $\bar{\mathbf{T}}$, of a suspension of rigid particles in a Newtonian medium is given by Batchelor (1970),

$$\bar{\mathbf{T}} = -p\,\bar{\mathbf{I}} + \eta(\nabla\mathbf{u} + \nabla\mathbf{u}^t) + \frac{1}{V}\sum_i \int_{s_i} \mathbf{T}\cdot\mathbf{n}(\mathbf{r}-\mathbf{r}_i)d^2\mathbf{r} \qquad (25.7)$$

where $\mathbf{T}$ is the local stress tensor. The summation is performed over all particles i contained in the reference volume V. The surface of the ith particle is denoted by s_i. The vector $\mathbf{r}_i$ indicates the center of the ith particle and $\mathbf{n}$ denotes the normal vector.

To be able to calculate the above integral, the stress distribution in the fluid surrounding the particles must be known. In a very dilute suspension the flow field and the stress distribution around a spherical particle can be calculated exactly. In the case of a concentrated suspension some approximations usually need to be made. The most simplifying approximation, applied in the case of concentrated suspensions where the particles nearly touch each other, is that the stress in the interstitial holes between particles is negligible compared to the stress generated in the narrow gaps separating particles (*i.e.*, only the nearly pairwise additive *lubrication* forces need be considered). The particle contribution to the stress tensor $\bar{\mathbf{T}}_p$ thus becomes (Goddard, 1977; van den Brule and Jongschaap, 1991)

$$\bar{\mathbf{T}}_p = \frac{1}{V}\sum_{i>j} \mathbf{f}_{ij}\,\mathbf{R}_{ij} \qquad (25.8)$$

where $\mathbf{f}_{ij}$ is the lubrication force acting between the ith and jth particles and the summation is carried out over all near pairs.

For specific configurations of particles, estimates of the effective viscosity of a suspension have been made assuming that only the normal direction portion of the lubrication force is important (Frankel and Acrivos, 1967) or including both the normal and shear components (van der Brule and Jongschaap, 1991). The latter compared favorably to an exact calculation of the viscosity of a periodic cubic array of spheres, taking into account all hydrodynamic interactions (Nunan and Keller, 1984) indicating that, at least in a cubic configuration, the lubrication forces do dominate the behavior at high concentrations.

25.1.4 Numerical Simulation of Complete Hydrodynamic Interactions

25.1.4.1 Quasi static Deformations -- Stokesian Dynamics

For particles suspended in a viscous fluid at zero Reynolds number (*i.e.*, Stokes) flow the linearized hydrodynamic equations can be solved throughout the space occupied by the fluid (and the particles). A set of "induced" forces can be applied to the fluid at the "surfaces" of the suspended particles to reproduce stick boundary conditions. The crux of the technique known as Stokesian dynamics is the computation of the induced forces that will reproduce the desired fluid velocity field that matches the surface motion of the translating, rotating particles. For spherical particles this is accomplished numerically by multipole moment expansions of particle-surface force distributions. In theory, any desired accuracy is obtainable by simply using higher moment approximations. In practice, the technique becomes computationally unwieldy as forces diverge. Significant efficiency is gained for high concentrations by calculating the short range lubrication forces between nearest-neighbor particles as separate pairwise forces; effectively utilizing the multipole expansion solutions primarily in the fluid outside the small "gap" regions. The method does not include inertial effects, and thus, is able to successfully avoid contacts or overlapping of spherical particles through the inclusion of diverging hydrodynamic lubrication forces. Brady (1992) discuses this method in detail in the next chapter; also, see Ladd (1990).

The Stokesian dynamics method generally has limited flexibility and is thus, difficult to extend to arbitrary particle shapes or to complex flow geometries. Also, the numerical algorithms usually scale as the square or even the cube of the system size, making simulations of large systems intractable. An alternative approach, with the potential to handle larger systems and more complex flow situations, is to utilize a lattice-gas cellular-automata model for the fluid motion combined with a moving-boundary algorithms for the suspended particles.

25.1.4.2 Low Reynolds Number Flows -- Lattice Gas Models

In a lattice-gas fluid space is filled with a fixed lattice of "sites" of which ~50% are "occupied" by lattice-gas (fluid) "particles". These particles move at fixed speed to adjacent sites and "collide" with other lattice-gas particles via micro-rules that conserve momentum and energy. Averages of velocities and concentration over several lattice sites reproduce Navier-Stokes fluid behavior (Frisch, *et al.*, 1986).

In suspension models using this approach a moving solid body (*i.e.*, a suspended particle) interacts with the lattice-gas via additional micro-rules which represent the collisions of the lattice-gas particles with the surface of the solid body (Ladd and Frenkel, 1990). On average these rules force the fluid next to the solid particle to move with the local velocity of the particle surface, modeling a hydrodynamic stick boundary condition. As a consequence, the lattice-gas particles exert forces and torques on the suspended particles which are then used to update the particle velocities and angular velocities, according to the masses and moments of inertia of the solid particles.

These models include inertial effects and appropriately handle lubrication force divergence for approaches up to a small fraction of a lattice cell spacing.

For dynamic situations and very close approaches, however, the approximate lubrication forces of the lattice-gas model are insufficient to prevent occasional overlapping of the particles. In such situations Ladd and Frenkel (1990) employ elastic hard-sphere (molecular dynamics) collision operators to prevent such overlaps. The method has the flexibility to include more complex interaction models for particle-particle collisions, such as the models described later in this chapter. Full hydrodynamic coupling between the fluid and the suspended particles is achieved and good agreement has been obtained with existing data on dissipative and fluctuating hydrodynamic interactions (Ladd, 1991). The method is computationally limited to flows with relatively high effective viscosities for the fluid, and thus, can only be applied to relatively small Reynolds' number flows.

25.1.4.3 Dynamic Flows -- Lattice Boltzman Models

Another method currently under development for suspensions (Ladd, 1992) is to utilize a lattice-Boltzman equation for the fluid (McNamara and Zanetti, 1988; Higuera, *et al.*, 1989; McNamara and Alder, 1992), with coupling between the phases handled analogous to the lattice-gas models. In this method the computational domain is divided into zones by a regular three-dimensional mesh; at each node a density of "fluid-like" particles is defined moving in a set of 18 lattice directions, corresponding to the nearest and second nearest neighbors of a simple cubic lattice. The population densities are a discretization in velocity space of the one-particle Boltzman distribution function. The hydrodynamic fields, mass density, momentum density and stress, are obtained directly as moments of this discrete distribution function.

The method was originally derived from lattice-gas models; however, it has several advantages over them. There are many fewer constraints on the choice of collision operators, allowing high Reynolds' number flows to be modeled. Recent lattice Boltzman simulations of a Kelvin-Helmholtz instability, at a Reynolds' number of 10000 were in near perfect agreement with a state-of-the-art Navier-Stokes solver (McNamara and Alder, 1992). The large statistical fluctuations present in a lattice-gas are absent in the lattice-Boltzman equation; thus, spatial or temporal averaging of the fluid dynamics is no longer necessary. The divergence of the lubrication forces is expected to be valid for gaps down to a fraction of a lattice grid spacing as it is for lattice-gas models. For closer approaches, or highly dynamic collisions, some additional particle-particle collision operator will need to be included.

The remainder of this chapter will discuss various approaches for modeling particle-particle interactions and/or collisions. To date macroscopic particle interaction models have been used primarily in simulations or theories of dry granular flows; however, they could also be added as supplementary collision operators for lattice-gas or lattice-Boltzman simulations of multi-phase flows. In the limit that the viscous effects of the fluid are negligible (*i.e.*, either Bagnold's grain-inertia regime, or extremely slow deformation where the gradients in velocity are small) the particle contribution to the stress tensor can dominate the stress and the deformation behavior. In truly quasi static situations with gravity and boundaries, particles will eventually settle to the point of physical contact with each other and the container walls. In such situations the continuous-contact soft-particle models discussed below could be used to prevent particles from "overlapping".

25.2 SIMULATION OF PARTICULATE SYSTEMS

Direct numerical simulation of particulate motions has been a viable research tool for the study of the macroscopic behavior of assemblies of *molecular-scale* particles for over 3 decades. The molecular-dynamics literature is extensive, with literally thousands of papers. Several recent books on the subject cover not only the history (Ciccotti and Hoover, 1986; Ciccotti et al., 1987) but also the methods (Hockney and Eastwood, 1981; Allen and Tildesley, 1987). Allen and Tildesley provide a thorough discussion of the details of the numerical techniques and "tricks of the trade" and include over 600 references. Also, Hoover (1991) discusses both classical statistical mechanics and modern computational approaches providing information on basic algorithms and advanced non-equilibrium and constrained-dynamics techniques.

Before any numerical simulation of particulate motion can be undertaken, the nature of the particle-particle interactions must be specified. In their simplest form particle-dynamics simulations consist of a set of "hard-spheres" following piece wise-linear trajectories between isolated momentum-conserving collisions. More complex simulations numerically integrate Newton's equations of motion to determine the trajectories as particles interact via short or long range forces. In general, the hard-sphere models are considerably faster than continuous force models. At high densities, however, hard-sphere collision frequencies increase dramatically and, when inelastic particles are simulated, care must be exercised to avoid situations where clusters "collapse" to a zero vibrational energy state wherein collision frequencies diverge as relative velocities vanish.

On a molecular scale a wide variety of energy-conserving force models have been utilized, ranging from repulsive power-law potentials to empirical functions approximating measured or *ab initio* calculated potential functions. The major difference between these molecular-scale interaction models and models used for macroscopic interactions is that, in a macroscopic collision, a portion of the incident kinetic energy is converted into either plastic work, deforming the particles' surfaces, or into molecular-scale thermal energy, during the collision process. As a consequence, inelastic (energy dissipating) collision models are employed to simulate macroscopic interactions. These can be rigid-body models or deformable 'soft' particles. For continuous-force 'soft'-particle models the energy absorption can take the form of a viscous damping or a hysteretic force-displacement path, in either the normal or tangential direction, or in both directions.

25.3 MACRO-SCALE ELASTIC AND INELASTIC CONTACTS

25.3.1 Hertzian Contacts and Impacts of Elastic Spheres

Hertz solved the linear elasticity equations for elastic bodies in contact (Hertz, 1881; Timoshenko and Goodier, 1970; Johnson, 1985). The resulting quasi static force displacement relation for displacements along the line of centers between two contacting, identical elastic spheres is given by

$$F = \frac{1}{3}\,\frac{E}{1-\nu^2}\sqrt{2R}\;\alpha^{3/2} \tag{25.9}$$

where E is Young's modulus, ν is Poisson's ratio, R is the spheres' radius, and α is the relative displacement after initial contact, (*i.e.*, the "virtual"

overlap of the two original spherical surfaces as the elastic spheres deform at the point of contact).

25.3.2 Elastic Spheres: Theory, Experiments and Finite Element Calculations of Impacts

It has been experimentally, theoretically and calculationally verified that, for low velocity normal-direction collisions between two elastic spheres, very little energy goes into acoustic or other vibrational internal energy inside the spheres; almost all of the initial kinetic energy is recovered in the post-collisional velocities. Walton and Hagen (1984) calculated the response of an elastic sphere impacting a rigid wall using the DYNA2D finite element code (Halquist, 1978). Figure 25-1 shows representative zoning for those calculations, which are equivalent to a head-on collision between two identical spheres. They found that if the yield strength is not exceeded in the contact region of the spheres, then 99% or more of the initial kinetic energy is recovered. For spheres of nearly equal size, the duration of the contact is usually any times the sound transit time across one of the spheres, so that the assumptions of Hertz's quasi static analysis are satisfied. The same finite element calculations confirmed that, for collisions between elastic spheres, the contact time varies nearly as the inverse 1/5 power of the relative impact velocity -- as would be predicted by the Hertz contact theory if Equation 25.9 represents the force-displacement behavior of a nonlinear spring acting between two rigid spheres (Timoshenko and Goodier, 1970),

$$\tau = 2.94 \left(\frac{5\sqrt{2}\pi\rho}{4} \frac{1-\nu^2}{E} \right)^{2/5} \frac{R}{v_n^{1/5}} \cdot \qquad (25.10)$$

where τ is the contact time, ρ is the density of the spheres and v_n is the incident relative velocity in the normal direction.

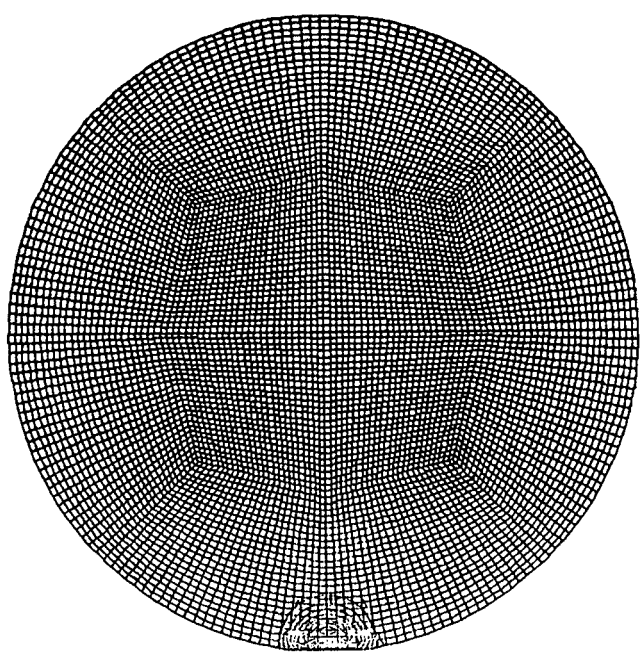

FIGURE 25-1 *Representative zoning used in dynamic finite element calculations of elastic and elastic-plastic spheres impacting a rigid wall (Walton and Hagen, 1984).*

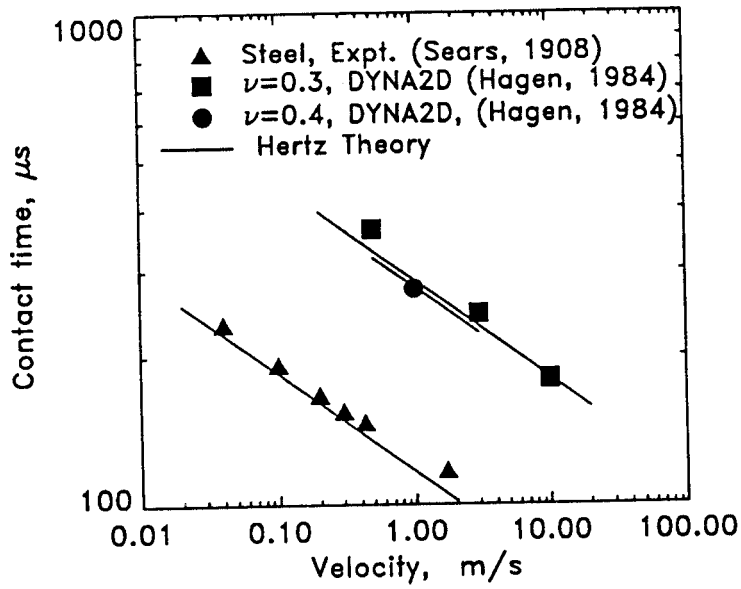

FIGURE 25-2 *Calculated contact time for impacts of elastic spheres, (Walton and Hagen, 1984), and measured contact times, for impacts of rods with spherical ends (Sears, 1908), compared with Hertz theory predicted inverse 1/5 power dependence on incident velocity, solid lines.*

Figure 25-2 shows the variation of contact time with impact velocity obtained in elastic finite element model calculations (Hagen and Walton, 1984), in experimental impacts of rods with spherical ends (Sears, 1908, as quoted in Goldsmith, 1960), and Hertz' contact theory (e.g. Equation 25.10). As can be seen, both the experiments and the finite element calculations are reasonably close to Hertz' contact theory, indicating that the quasi static assumptions of that theory are nearly satisfied in these elastic collisions.

25.3.3 Inelastic Spheres: Calculation of Elastic-Plastic Contact Forces and Impacts

There is ample experimental, theoretical and calculational evidence that for any substantial impact velocity between two colliding spheres, yield strengths will be exceeded in the contact area and significant energy will go into irreversible work deforming the surfaces in the region of contact (Goldsmith, 1960). Walton and Hagen (1984) repeated their elastic sphere finite element calculations using an elastic-perfectly-plastic constitutive model. The yield strength for these generic calculations was arbitrarily set to match the maximum calculated deviatoric stress in the contact region during a previously calculated elastic impact with an incident velocity of 0.3 m/s. For impacts at speeds less than this 'plastic yield threshold' value, the elastic-plastic results were essentially identical with the previous perfectly-elastic calculations, with less than 1 percent of the initial kinetic energy being lost upon recoil, either to numerical error or elastic waves inside the rebounding spheres. For velocities exceeding the threshold where plastic flow developed in the contact region, the effective coefficient of restitution, e, (defined as the negative of the ratio of

recoil to incident speeds) falls approximately as the inverse 1/4 power of the velocity; a relation proposed for fully plastic collisions (Johnson, 1986).

The calculations were repeated with a slightly higher yield strength, set to allow plastic flow to initiate at an impact velocity of 0.5 m/s. These calculations produced similar results. Figure 25-3 shows the coefficient of restitution obtained in these calculations and representative experimental values obtained for collisions between ductile metal spheres (Goldsmith, 1960). Also shown on this Figure is the behavior of the empirical 'partially latching spring' model of Walton and Braun (1986).

Most discrete particle simulation calculations to date have used a constant coefficient of restitution, independent of incident velocity. The primary reason for using a fixed value for e is that most kinetic theory models of granular flow also employ a constant value for e, and there are very few experimental results available that include sufficient measurements of collision properties to adequately characterize the coefficient of restitution, except by a single average value, valid in the range of velocities observed in the experiments.

The same elastic and elastic-perfectly-plastic constitutive models were used in quasi static finite-element calculations to determine the effective normal-force displacement behavior for this idealized configuration (Walton

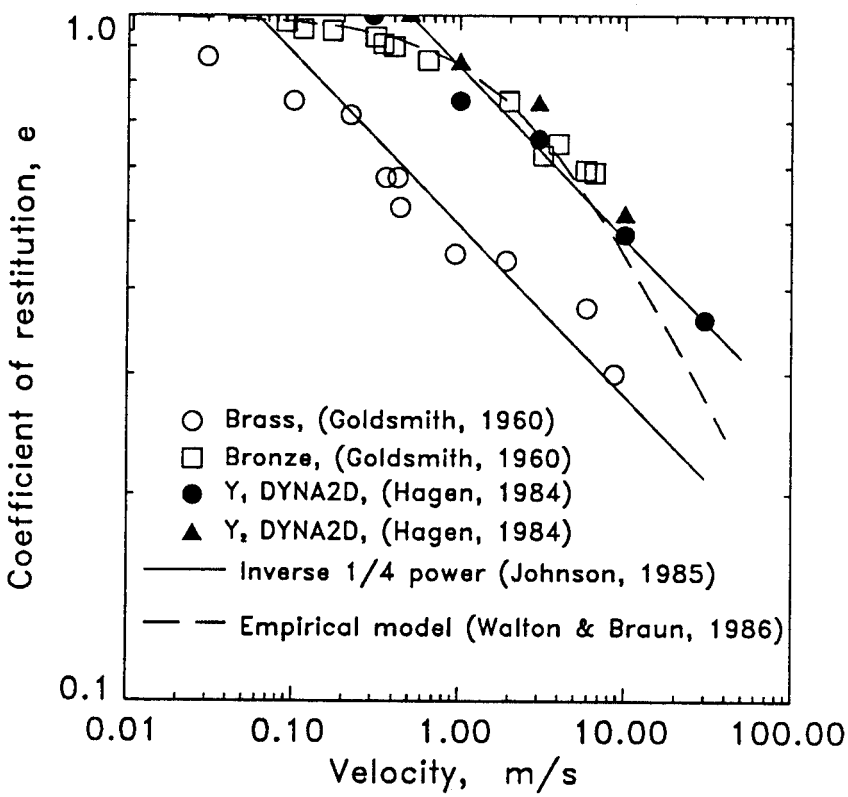

FIGURE 25-3 *Variation of coefficient of restitution with impact velocity. Experimental results (open symbols) are for metal spheres (Goldsmith, 1960). Finite element calculations for elastic perfectly-plastic material model are shown as filled circles (yield strength set so plastic deformation starts at impact velocities exceeding 0.3m/s) and pluses (yield set to allow plastic deformation only above 0.5m/s). Dashed line is representative curve for empirical formula of Walton and Braun (1986). Solid lines are inverse 1/4 power of velocity, as predicted by fully plastic theory (Johnson, 1986).*

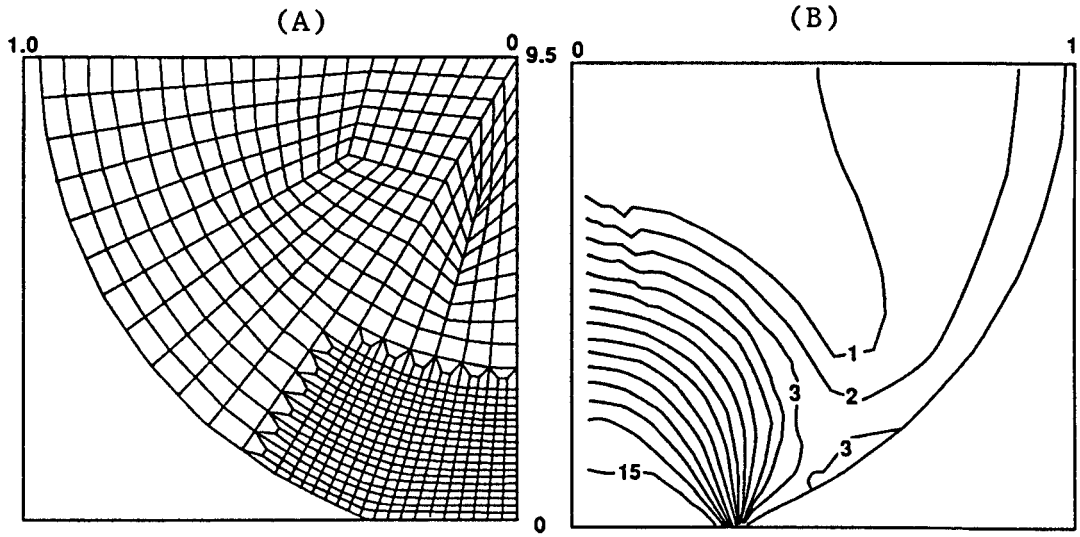

FIGURE 25-4 *a) Representative zoning used in finite element calculations of a hemisphere impinging on a rigid wall (Walton and Brandeis, 1984), and b) Calculated equal pressure contours using elastic-perfectly-plastic constitutive model.*

and Brandeis, 1984). Figure 25-4a shows representative zoning used in these axisymmetric, two-dimensional calculations utilizing the NIKE2D finite element model (Halquist, 1979). Coarser and finer meshes were also used. Since most of the deformation was localized in the contact region only the contacting half of the sphere was modeled. Using a perfectly-elastic constitutive model in the calculations, Walton and Brandeis verified that, to within one or two percent, the finite element force-displacement curve followed the predicted Hertzian 3/2 power relationship given by Equation 25.9.

Using an elastic-perfectly-plastic constitutive model in the NIKE2D code, the hemisphere was moved, in successive steps, toward the wall, withdrawn, and then back toward the wall again, to produce loading, unloading and reloading force-displacement curves. Figure 25-4b shows contours of constant pressure near the maximum indentation experienced by the elastic-plastic hemisphere. Figure 25-5 shows the resulting quasi-static force displacement behavior for the *elastic-plastic* body compared to the theoretical *elastic* Hertzian 3/2 power force-displacement curve. The wavy character of the elastic-plastic loading curve appears to be the result of the coarseness of the finite element mesh. When coarser or finer elements were used, the general nearly-linear loading curve was reproduced; but, the magnitude of the "wiggles" on the curve scaled with the zone size. It appears that as each new annular zone comes into contact with the rigid planer surface it initially responds elastically (*i.e.*, nearly like the theoretical Hertzian curve) but, as the elastic limit is reached and plastic flow occurs in the newly loaded zone, the force *vs.* displacement curve exhibits a lower slope until the next annular zone starts bearing a significant fraction of the load, etc. The dashed

line on Figure 25-5 is a straight line drawn approximately through the 'average' calculated force-displacement loading curve.

Nearly linear loading behavior for plastically deforming contacts of spherical surfaces has also been observed experimentally. Goldsmith (1960) reports similar behavior measured during impacts of a steel sphere on an aluminum rod with a spherical end. Mullier, *et al.* (1991) measured normal-direction force *vs* micro-displacement for 6mm diameter cellulose acetate spheres in contact. While they report fitting a 3/2 power curve to the data, subsequent analysis done by Drake and Walton (1992) has inducted at least as good a fit to the observed data with a linear loading curve. Also, scanning electron microscope (SEM) examination of the contact surface region of these cellulose acetate spheres showed evidence of plastic deformation.

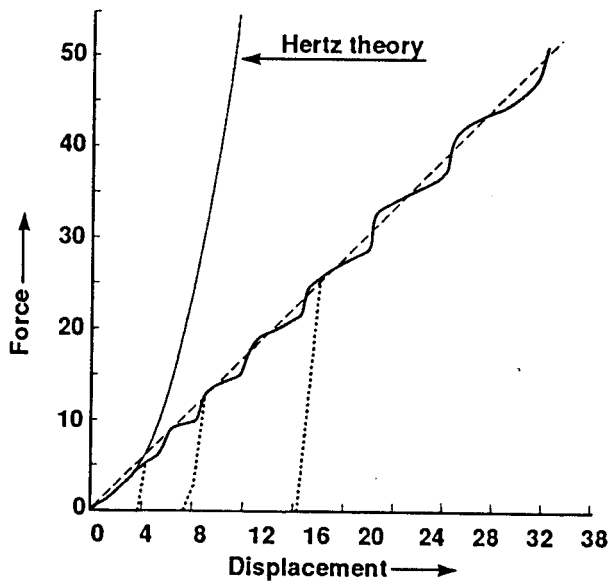

FIGURE 25-5. *Loading and unloading force-displacement behavior for elastic-plastic spheres during quasi static normal displacement as calculated using NIKE2D finite element model (Walton and Brandeis, 1984)*

25.3.4 Hysteretic Normal Force Models

Walton and Braun (1986) use a simple empirical normal force model that approximates the behavior observed in the above experiments and finite element calculations. In their model the normal force has a linear loading curve, with a slope K_1, and a steeper linear unloading slope, K_2. The normal force, N, is given by,

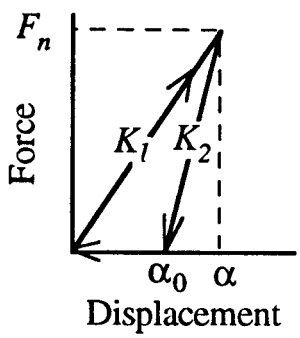

FIGURE 25-6

$$N = \begin{cases} K_1\alpha & \text{for loading, and} \\ K_2(\alpha - \alpha_0) & \text{for unloading.} \end{cases} \qquad (25.11)$$

Unloading follows this steeper slope until the normal force is zero (with a finite "overlap," α_0, remaining). Upon further unloading the force remains at

zero, or, upon reloading, it increases with slope K_2 until the original loading curve (K_1) is reached, (see Fig. 25-6). The slope of the unloading/reloading curve, K_2, can be set to increase linearly with the maximum force reached during a contact, or it can be set to a constant value. The area between the loading and unloading paths represents the energy lost to plastic deformation. If the unloading slope K_2 is a fixed value (independent of the past load history) then a constant coefficient of restitution given by $e = \sqrt{K_1/K_2}$ results for this model. If the unloading slope, K_2, is allowed to increase linearly with the magnitude of the maximum force ever experienced by the contact (e.g., $K_2 = K_0 + S\, F_{max}$) where the slope factor, S, is a fixed model parameter, empirically determined, then the coefficient of restitution behavior is as shown in Figure 25-3. Similar models can be easily constructed using non-linear (e.g. Hertzian-like) loading and unloading paths, by simply changing the power of the displacement terms in Equation 25.11. If the displacement terms are raised to the 3/2 power in Equation 25.11, then the initial loading is the same form as Hertz' elastic solution and the coefficient of restitution is given by $e = \sqrt[3]{K_1/K_2}$.

25.3.5 Visco-elastic Normal Force Models

An alternative to a position dependent contact model is to utilize a viscous damping term to dissipate energy. The damping can be added to an otherwise elastic normal force model. A linear damped harmonic oscillator is the simplest such approach, letting the normal force, N, be given by

$$N = K\,\alpha + D\,\dot{\alpha} \tag{25.12}$$

where K and D are constants., and α and $\dot{\alpha}$ are the relative normal displacement and velocity at the contact point. Such a model produces a constant coefficient of restitution, independent of impact velocity. As usually implemented, however, the force is purely repulsive and the viscous term is set to zero whenever there is no overlap (see, Cundall, 1974 and 1979). Such an approach leads to a discontinuity in the force as initial contact (*i.e.*, overlap) is established since $\dot{\alpha}$ is a maximum when $\alpha = 0$. The discontinuity can be eliminated by "weighting" the viscous term by the displacement. A general power law relation

$$N = K\,\alpha^n + D\;\alpha^m\,\dot{\alpha} \tag{25.13}$$

has been proposed to model real inelastic contacts (Hunt and Crossley 1975, Oden and Martins 1984). Such a power law relationship can be Hookeian (*i.e.*, with n =1) or Hertzian (n = 3/2) and can have a discontinuity on initial contact (m = 0) or it can have the damping "weighted" by the elastic force (m = n). For implementation, the values of all four parameters K, n, D and m need to be determined empirically. Oden and Martins (1984) discuss the energy losses obtained with such a model.

25.4 FRICTIONAL CONTACTS

25.4.1 Analysis of Frictional, Elastic Contacts

The problem of arbitrary oblique contacts between two frictional elastic spheres has never been completely solved. Despite the fact that more than 100 years have passed since Hertz solved the linear elastic contact equations for the distribution on normal-direction stress and strain in the region where two elastic spheres contact each other, there is still no complete solution to the stress and strain distribution if Coulombic friction is assumed to apply on the contact surface, and arbitrary rotation and tangential sliding are combined with changing normal direction contact between elastic spheres. Mindlin (1949) derived expressions for tangential compliance *vs* displacement for spheres with elastic Hertzian normal stress distributions in their contact regions. The resulting force *vs* displacement relationship is of the form

$$F = \mu N \left[1 - \left(1 - \frac{16Ga}{3(2-\nu)\mu N} \delta s \right)^{3/2} \right] \qquad (25.14)$$

up to the full sliding limit at $\delta s = \frac{3(2-\nu)}{16Ga} \mu N$ when the entire contact experiences slip and the tangential force is just equal to the Coulomb friction limiting value, $F = \mu N$; where G is the shear modulus, ν is Poisson ratio, N is normal load, μ is the coefficient of friction, δs is tangential displacement and a is the Hertzian contact radius given by

$$a = (E^* N R)^{1/3}$$

where $E^* = \frac{3}{2}\left(\frac{1-\nu^2}{E}\right)$, and E is young's modulus.

If contacting spheres simultaneously experience rotation, either about their contact normal, or "rolling," coupled with tangential sliding, then the tangential strain distribution is modified and Mindlin's theory does not adequately describe the tangential force or compliance. Various approximate models, that are relatively straight forward to calculate, have been proposed for frictional contacts such as the "elastic bed" normal force model combined with a "wire brush" tangential friction model (see Johnson, 1990) and an "incrementally slipping" model approximating Mindlin's tangential functional form for initial tangential loading (Walton and Braun, 1986; Walton, 1992). It is beyond the scope of this chapter to thoroughly review various "soft" particle friction models; however we will examine the nature of the rotational coupling that occurs for binary collisions between frictional spheres -- the feature most relevant for numerical models of granular flow. The reader is referred to Johnson (1985), and Oden and Martins (1984) for further discussion on frictional contact models. Also, Thornton (1988) and Patrakas *et al* (1990) have implemented numerical algorithms that approximate Mindlin and Deresiewicz (1953) force-displacement behavior for simultaneous tangential and normal direction displacements. (These models still do not include the confounding effects of rotations on the stress distribution in the contact region).

25.4.2 Experiments and Numerical Analysis of Frictional Collisions

Experiments involving carefully controlled impacts of an air table "puck" (made from a section of a sphere) with a planar wall, demonstrate that release of tangential elastic strain energy stored during a collision can, indeed, reverse the direction of the original rotation and the relative surface velocity at the contact point (Maw *et al.*, 1976, 1981). This is a phenomenon familiar to anyone who has played with a "superball" (e.g. see Garwin,1969), and corresponds to positive values of Lun and Savage's (1987) parameter, β, discussed below.

Maw *et al* numerically integrated the tangential stress over a Hertzian contact area during collisions that involved both sliding and rotation. Their numerical solution to the frictional contact problem was essentially equivalent to Mindlin's analysis of oblique contacts between elastic spheres (Mindlin, 1949; Mindlin and Deresiewicz, 1953). They assumed that the tangential surface displacement due to either rotation or sliding had identical effects on the distribution of tangential stress in the circular contact area (equivalent to assuming the displacement is all effectively "sliding"). This approach ignores "rolling" resistance that occurs even when no relative surface velocity exists, but both spheres are counter rotating so that their surfaces "roll" on each other and also ignores any effects due to rotation about the contact normal. Nonetheless, Maw *et al's.* analysis was able to capture the most important physical phenomena for impacts restricted to a plane. Their careful numerical integration of the contact forces acting between frictional, elastic spheres, demonstrated that the degree of tangential coupling depends strongly on the ratio of the effective tangential-direction stiffness to the stiffness in the normal-direction (Maw *et al.* 1981).

The continuously varying contact force models used in most discrete particle simulations such as Cundall (1974), Cundall and Strack(1979), Walton and Braun (1986a and Walton (1992) automatically allow reversal of the tangential surface velocity as tangential strain energy is recovered during rebound. No explicit assumptions are made in such models about rotational restitution coefficients; however, depending on the ratio of tangential to normal stiffnesses assumed, behavior very similar to that predicted by Maw *et al* can be obtained in these simulated collisions (see Walton & Braun, 1986a).

25.5 HARD SPHERE COLLISIONS WITH FRICTION

In the interest of computational efficiency, it is often preferable to specify an instantaneous collision operator for rigid particles instead of evaluating a continuously varying force-displacement relationships 40 or 50 times during each collision in the simulation. Such hard-sphere collision operators are also utilized in kinetic theory models of granular flow. Various models have been proposed to approximate collisions between inelastic, frictional spheres.

On a molecular scale perfectly rough, perfectly elastic, spheres have been a standard, energy conserving, model for molecules that include rotational degrees of freedom for decades (Chapman and Cowling 1952). More recently, various partially rough collision models have been proposed (e.g., Berne, 1977; Veseley, 1980); however, since these models conserve energy, they are not appropriate for modeling interactions between macroscopic sized

particles that collide inelastically and with sliding friction. Goldsmith (1960) describes the usual model assumed for *frictional* impacts (*i.e.*, that friction forces can only slow or stop the relative tangential velocity between colliding particles). Two-dimensional hard-disk simulation models such as Hawkins(1983) and theoretical models such as Nakagawa (1987) utilize collision operators that are equivalent to Goldsmith's treatment, combined with a non-unity coefficient of restitution in the normal direction. Others, such as Campbell and Brennen (1985), have assumed that all collisions result in zero relative surface velocity upon disengagement (*i.e.*, all contacts are rolling contacts). Brach (1988) utilizes a coefficient, μ, to characterize the tangential momentum transferred in oblique impacts. His model can allow the direction of rotation to reverse, but his single parameter is not directly related to contact friction and is difficult to calibrate against measured properties.

Lun and Savage (1987) describe a rough, inelastic sphere collision operator incorporating a rotational restitution coefficient, β, defined analogous to the normal direction coefficient of restitution, e. According to their rough inelastic sphere model, two particles of diameter σ, having translational velocities $\mathbf{v}_1$ and $\mathbf{v}_2$, angular velocities $\vec{\omega}_1$ and $\vec{\omega}_2$, have a total relative velocity, $\mathbf{g}_{12}$, at their contact point just prior to collision given by,

$$\mathbf{g}_{12} = \mathbf{v}_{21} - \frac{\sigma}{2}(\hat{\mathbf{r}}_{12} \times \vec{\omega}_{12}) \tag{25.15}$$

where $\hat{\mathbf{r}}_{12}$ is a unit vector from particle 1 to 2, $\vec{\omega}_{12} = \vec{\omega}_1 + \vec{\omega}_2$, and $\mathbf{v}_{21} = \mathbf{v}_1 - \mathbf{v}_2$. During a collision the components of velocity and angular velocity are changed such that,

$$\hat{\mathbf{r}}_{12} \cdot \mathbf{v}'_{21} = -e\ (\hat{\mathbf{r}}_{12} \cdot \mathbf{v}_{21}) \tag{25.16}$$

and

$$\hat{\mathbf{r}}_{12} \times \mathbf{g}'_{12} = -\beta\ (\hat{\mathbf{r}}_{12} \times \mathbf{g}_{12}). \tag{25.17}$$

where the prime indicates the post-collision values and they assume the coefficients e and β are fixed constants in the ranges, $0 \le e \le 1$ and $-1 \le \beta \le 1$, with $\beta = -1$ being perfectly smooth, $\beta = 1$ perfectly rough spheres (Chapman and Cowling, 1952), and $\beta = 0$ corresponding to Campbell and Brennen's (1985) rolling contact model. Fixed values for e and β were used by Lun and Savage to represent average values over a spectrum of collisions and served to allow sensitivity of stresses to inelasticity and roughness to be studied, but there was no direct correspondence between rotational restitution coefficient, β, and a contact friction coefficient.

25.5.1 Frictional Hard-Sphere Collision Operator

A more realistic inelastic, frictional collision operator can be described using three parameters:

1) the coefficient of restitution, e, in the normal direction;
2) a coefficient of rotational restitution, β_0, for those contacts that are not continuously sliding during the entire collision, and,
3) a coefficient of sliding friction, μ, acting during sliding or grazing collisions.

The model is essentially an extension of the disk collision operators of Hawkins(1983) or Nakagawa (1987) or Hopkins (1988) to three dimensions

with the additional feature that, during a collision, tangential velocity differences can not only decrease, but can also reverse direction. This three parameter model provides a reasonably accurate description of collisions between real macroscopic spheres, and it can easily be extended (by making β into a function of the angle of incidence) to be nearly an exact representation of collisions between frictional, elastic spheres interacting with Hertz-Mindlin contacts (see Mindlin, 1949; Maw *et al.* 1976, 1981; Walton and Braun, 1986a; or Walton, 1992).

Consider a collision between two frictional, inelastic spheres with mass m_a and m_b, centers located at $\mathbf{r}_a$ and $\mathbf{r}_b$, traveling with velocities $\mathbf{v}_a$ and $\mathbf{v}_b$ before impact and having rotational velocities $\vec{\omega}_a$ and $\vec{\omega}_b$. Let,

$$\hat{\mathbf{r}}_{ab} = \frac{\mathbf{r}_b - \mathbf{r}_a}{|\mathbf{r}_b - \mathbf{r}_a|} = \text{unit vector from } a \text{ to } b,$$

$$\mathbf{v}_{ab} = \mathbf{v}_b - \mathbf{v}_a = \text{relative velocity},$$

$$v_n = \mathbf{v}_{ab} \cdot \hat{\mathbf{r}}_{ab} = \text{normal component of relative velocity},$$

$$\mathbf{v}_n = v_n \hat{\mathbf{r}}_{ab} = \text{normal direction relative velocity},$$

$$\mathbf{v}_t = \hat{\mathbf{r}}_{ab} \times (\mathbf{v}_{ab} \times \hat{\mathbf{r}}_{ab}) = \mathbf{v}_{ab} - \mathbf{v}_n = \text{tangential direction relative velocity},$$

$$\mathbf{v}_s = \mathbf{v}_t + \frac{\sigma_a}{2}(\hat{\mathbf{r}}_{ab} \times \vec{\omega}_a) + \frac{\sigma_b}{2}(\hat{\mathbf{r}}_{ab} \times \vec{\omega}_b) = \text{relative surface velocity (tangential direction)}$$

$$\hat{\mathbf{k}}_s = \frac{\mathbf{v}_s}{|\mathbf{v}_s|} = \text{unit vector in direction of incident surface velocity}$$

$$v_s = \mathbf{v}_s \cdot \hat{\mathbf{k}}_s = \text{tangential component of relative surface velocity}.$$

Conserving translational momentum and utilizing the usual definition of the coefficient of restitution, $e \equiv -v'_n/v_n$, and defining the rotational restitution coefficient as, $\beta \equiv -v'_s/v_s$, where the prime denotes post collision values, we obtain the changes in normal direction velocities,

$$\Delta \mathbf{v}_{na} = \frac{m_b(1+e)}{m_a + m_b}\mathbf{v}_n \tag{25.18}$$

$$\Delta \mathbf{v}_{nb} = \frac{-m_a(1+e)}{m_a + m_b}\mathbf{v}_n \tag{25.19}$$

Conserving angular momentum about the contact point we obtain three vector equations relating the four vector quantities giving the changes in rotational velocities $\vec{\omega}_a$ and $\vec{\omega}_b$ and the tangential direction translational velocities $\mathbf{v}_{ta}$ and $\mathbf{v}_{tb}$,

$$\Delta \vec{\omega}_a = \frac{2}{K\sigma_a}\hat{\mathbf{r}}_{ab} \times \Delta \mathbf{v}_{ta} \tag{25.20}$$

$$\Delta \vec{\omega}_b = \frac{2}{K\sigma_b}\hat{\mathbf{r}}_{ab} \times \Delta \mathbf{v}_{tb} \tag{25.21}$$

$$\Delta \mathbf{v}_{tb} = -\frac{m_a}{m_b}\Delta \mathbf{v}_{ta} \tag{25.22}$$

where $K = 4I_o/m\sigma^2 = 2/5$ or uniform density spheres and I_o is the moment of inertia. In order to solve for these four vector quantities an additional vector relation is needed. We use two forms for the fourth relation depending on the conditions of the impact -- one for *sliding* contacts and one for *rolling* contacts.

During frictional impacts the tangential force is always equal to or less than the product of the coefficient of friction, μ, and the normal force acting at the contact. The *sliding* solution assumes that during the entire contact the tangential force is always at the friction limit so that,

$$\text{(tangential impulse)} = \mu \text{ (normal impulse)}.$$

However, the assumption of fully sliding contacts is not always valid since sliding may dissipate sufficient energy for the two spheres to lose all relative tangential velocity (*i.e.*, to be rolling together). In real collisions relative tangential velocities can not only go to zero, but the stored tangential strain energy in the contact region can often cause the direction of the relative surface velocity to actually reverse before separation, leading to positive values of β (e.g., see Maw *et al.* 1976, 1981; and Drake, 1988).

The solution procedure consists of assuming a *sliding* contact, obtaining the changes in tangential and rotational velocities, then checking to see if the rotational restitution coefficient resulting from the sliding solution, β^*, given by

$$\beta^* = -1 + \mu(1+e)\left(1+\frac{1}{K}\right)\frac{v_n}{v_s} \quad \text{(sliding solution)}, \tag{25.23}$$

exceeds a predetermined (constant) maximum value, β_o, where $1 \geq \beta_o \geq 0$. If $\beta^* > \beta_o$, then a *rolling* solution equivalent to Lun and Savage's collision operator with a fixed $\beta = \beta_o$ is employed to determine the post collision velocities.

25.5.2 Numerical Implementation of Collision Operator

A numerical algorithm implementing this model for equal size, equal mass, inelastic, frictional spheres is as follows:

$$\hat{\mathbf{r}}_{ab} = \frac{1}{\sigma}(\mathbf{r}_b - \mathbf{r}_a) \quad \text{(at contact)}$$

$$\mathbf{v}_{ab} = \mathbf{v}_b - \mathbf{v}_a$$

$$v_n = \mathbf{v}_{ab} \cdot \hat{\mathbf{r}}_{ab}$$

$$\mathbf{v}_t = \mathbf{v}_{ab} - v_n \hat{\mathbf{r}}_{ab}$$

$$\mathbf{v}_s = \mathbf{v}_t + \frac{\sigma}{2}\hat{\mathbf{r}}_{ab} \times \left(\vec{\omega}_a + \vec{\omega}_b\right)$$

if $(\mathbf{v}_s \cdot \mathbf{v}_s) = 0$ then

$$\beta = -1$$

else

$$(1+\beta^*)^2 = \mu^2 (1+e)^2 \left(1+\frac{1}{K}\right)^2 \frac{v_n^2}{\mathbf{v}_s \cdot \mathbf{v}_s}$$

if $(1+\beta^*)^2 > (1+\beta_o)^2$ then

$$\beta = \beta_o \qquad \text{(rolling solution)} \qquad (25.24)$$

else

$$\beta = \beta^* \qquad [\text{ sliding solution} = -1+\sqrt{(1+\beta^*)^2}\ ]$$

endif

endif

where the sliding solution evaluation of β^* is the only step that requires a square root call. The resulting changes in normal, tangential and rotational velocity components for each sphere are given by,

$$\Delta \mathbf{v}_{na} = -\Delta \mathbf{v}_{nb} = \frac{1}{2}(1+e)\, v_n \hat{\mathbf{r}}_{ab} \qquad (25.25)$$

$$\Delta \mathbf{v}_{ta} = -\Delta \mathbf{v}_{tb} = \frac{K(1+\beta)}{2(K+1)}\, \mathbf{v}_s \qquad (25.26)$$

$$\Delta \vec{\omega}_a = \Delta \vec{\omega}_b = \frac{(1+\beta)}{\sigma(K+1)}\, \hat{\mathbf{r}}_{ab} \times \mathbf{v}_s \qquad (25.27)$$

The effect of this frictional, inelastic hard-sphere collision operator can be plotted as two straight lines giving the effective rotational restitution coefficient, β, as a function of the ratio of incident normal to tangential velocities, v_n/v_s, as shown on Figure 25-7 (e.g., Equations 25.23. and 25.24).

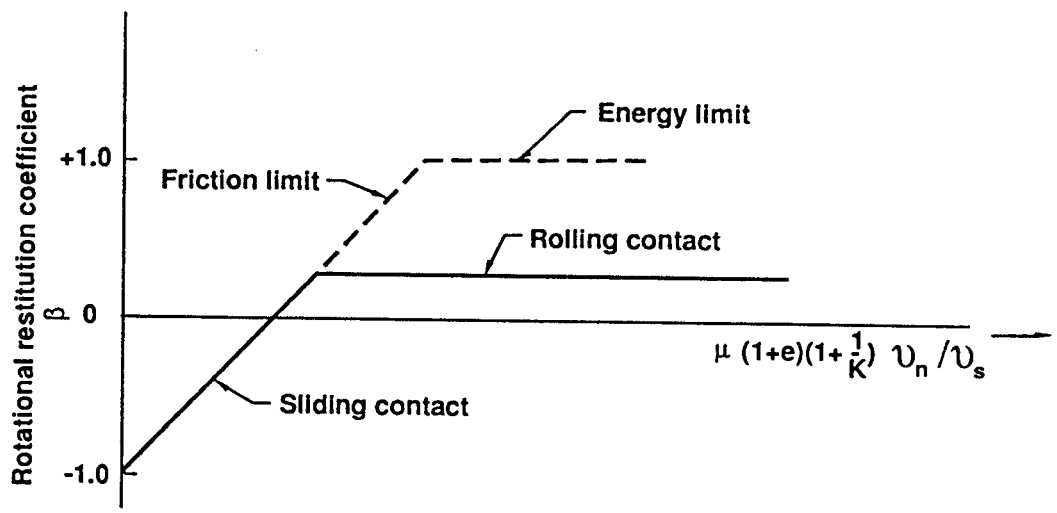

FIGURE 25-7 *Representative curve for rotational restitution coefficient, β, as given by the inelastic frictional collision operator (i.e., Equations 25.23 and 25.24).*

Application of the operator also produces two straight lines if plotted as the tangent of the effective recoil angle, $-v_s'/v_n'$, *vs* the tangent of the effective incident angle, v_s/v_n, as shown in Figure 25-8, which is equivalent to the ψ_2 *vs.* ψ_1 plots of Maw *et al.* (1976,1981). The rolling solution line in Figure. 25-8 is determined by the equation,

$$\frac{-v'_s}{v'_n} = -\frac{\beta_o}{e}\frac{v_s}{v_n} \quad . \tag{25.28}$$

and the equation for the sliding solution line on Figure. 25-8 is,

$$\frac{-v'_s}{v'_n} = -\mu\left(1+\frac{1}{e}\right)\left(1+\frac{1}{K}\right)+\frac{1}{e}\frac{v_s}{v_n} \tag{25.29}$$

The slightly deformable particle models of Walton and Braun (1986), the experimental measurements and analysis of sphere-wall collisions of Maw *et al.* (1976, 1981), and the measurements of Drake (1988), all show a similar character for collisions of frictional spheres, with the transition from sliding to rolling occurring less abruptly for real spheres than for the collision operator model. Drake's data for plastic sphere impacts indicate that a value of β_o near 0.35 is reasonable for the "rolling" branch.

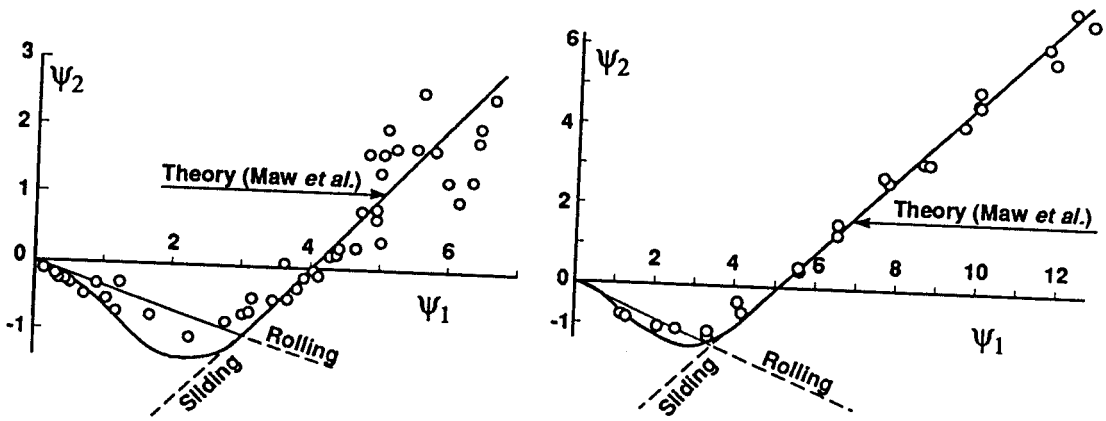

FIGURE 25.8 *Representative curves for tangent of effective recoil angle, $-v'_s/v'_n$, (i.e., ψ_2) vs. tangent of effective incident angle, v_s/v_n, (i.e., ψ_1) as determined by inelastic collision operator (equations 25.28 and 25.29), straight lines, by numerical analysis of Maw et al., solid curves, and in experiments of Maw et al. with rubber and steel (1976, 1981) symbols.*

25.6 STRESSES IN STEADY SHEARING FLOWS

Numerous numerical simulation studies of rapidly flowing dry granular solids have been performed over the past decade (e.g. see Campbell, 1990). Among other parameters examined, the stress tenser, given by a time average of the expression in Equation 25.6, has perhaps been the most thoroughly examined. For systems of *inelastic* particles that are at a packing density below that which produces continuous contacts (around 0.5) the

equilibrium stress is zero since, for dissipative systems, the equilibrium *state* has no kinetic energy. Granular material in steady shearing flow, on the other hand, is not at equilibrium and numerical simulations have confirmed Bagnold's analysis that in the *grain inertia* regime all stress tensor components vary with the square of the strain rate and particle size and directly with the density of the solid material. Most steady shearing flow results are non-dimensionalized by dividing the stress by $\sigma^2\rho_s\dot{\varepsilon}^2$ where σ is the particle diameter, ρ_s is the material density and $\dot{\varepsilon}$ is the strain rate.

Numerical simulations have corroborated kinetic theory predictions that show strong sensitivity to packing fraction and coefficient of restitution (see for example Walton and Braun, 1986a, 1986b; Walton, 1990). Initially unexpected, but later included in improved kinetic theories, were the large first normal stress differences found in steady shearing flows at very low solids fractions (Walton, Kim and Rosato, 1990). Other effects such as sensitivity to friction and recently observed clustering phenomena at low solids packing are currently the subjects of ongoing research efforts.

We have utilized the rigid sphere model to examine the effects of coefficient of friction, μ, and the maximum rotational restitution coefficient, β_o on stresses in rapid shearing flows of frictional spheres. Figure 25.9 shows how stresses in simulations at two different solids packings, $\nu = 0.4$ and 0.5, depend on coefficient of friction, μ, in the range, $0 \le \mu \le 1$, (stresses shown on this figure have been non-dimensionalized by dividing by $\sigma^2\rho_s\dot{\varepsilon}^2$). The results of three different rotational coupling assumptions are shown on this figure. The curves for solid packing of 0.4 and the dashed curve at the higher density are from simulations with 125 slightly deformable, equal-sized, inelastic spheres, using an incrementally-slipping friction model (Walton and Braun, 1986a, Walton, 1992). The coefficient of restitution for all interactions in this calculational series was 0.8. The stiffness of the slightly-deformable spheres (*i.e.*, K_1 in Equation 25.11) was selected so that maximum "overlaps" were a fraction of one percent of a sphere radius. This stiffness was varied by one order of magnitude to demonstrate that the results were insensitive to the specific value selected. The stresses calculated using spheres with the highest stiffness were generally within 2 percent of the values obtained with the hard sphere model (without friction).

The calculated non-dimensional normal stress, P^*_{yy}, was found to decrease monotonically with increasing friction at a packing fraction of $\nu = 0.4$. This is apparently because friction adds another energy loss mechanism, reducing the vibrational kinetic energy in the system, and thus, the stresses. However, the additional shear coupling between colliding particles compensates somewhat for this effect in the shear direction so that the shear stress is almost unaffected by the value of friction coefficient at a solids packing of $\nu = 0.4$ Although not shown on this figure, representative calculations were done at $\mu = 0.4$ with the hard-sphere model as well. They were generally within 2% of the values shown for the slightly deformable (*i.e.*, soft) sphere model.

At the higher density the results are more interesting, with the slightly-deformable model producing normal stresses that first decrease, then increase, as the coefficient of friction increases, and shear stresses that increase nearly monotonically with the coefficient of friction. The hard-sphere model with $\beta_o = 0.3$ shows the same qualitative behavior, but the increase in stresses is much more rapid as the coefficient of friction increases

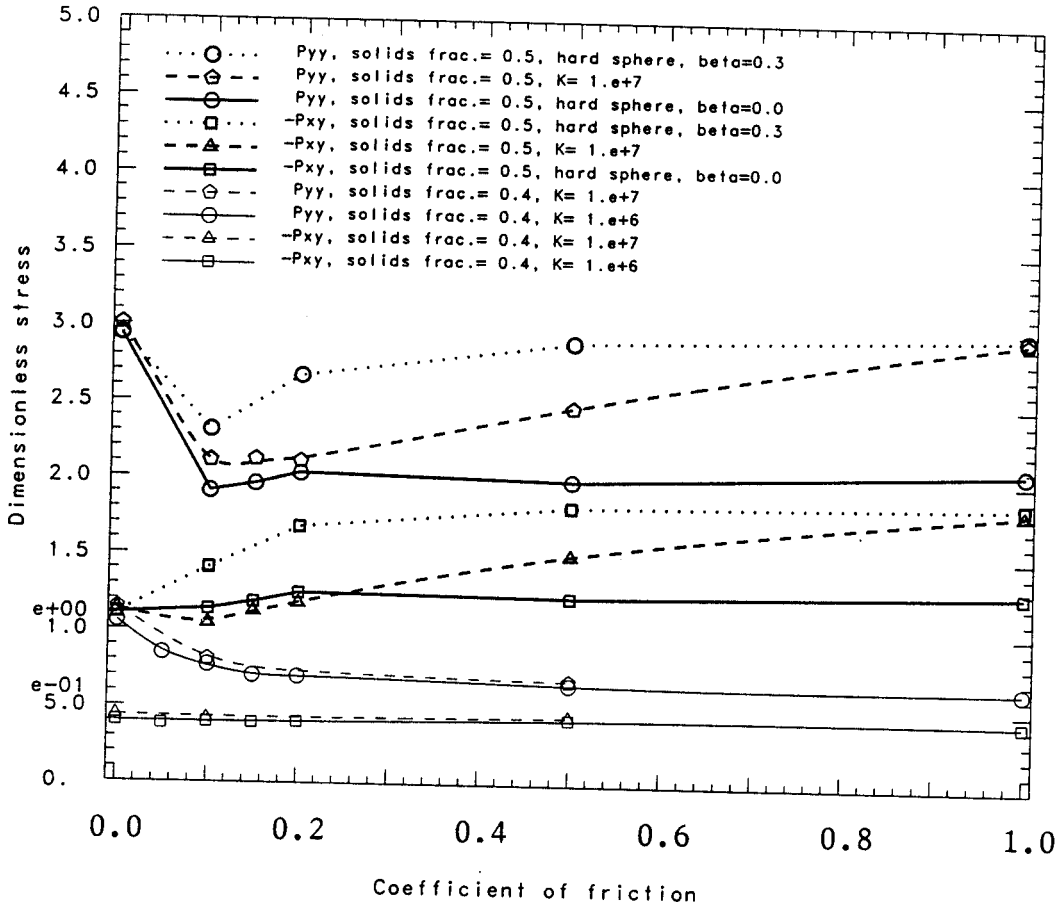

FIGURE 25-9 *Effect of coefficient of friction on non-dimensional shear and normal stresses in steady shearing flow of uniform sized, inelastic, frictional spheres as calculated for 108 hard spheres with two choices of the maximum rotational restitution coefficient, β_o, and for 125 slightly deformable spheres interacting with an incrementally-slipping friction model (Walton, 1992) similar in effect to that of Mindlin and Deresiewicz [1953].*

from 0.1 to 0.5. The hard-sphere model with $\beta_o = 0$ (corresponding to Nakagawa's model) does not show a significant increase in either stress component with increasing friction coefficient. Instead, the curves are qualitatively similar to those at the lower density. In almost all cases the stresses calculated by the incrementally-slipping deformable-sphere model lie between the two hard-sphere cases of $\beta_o = 0$ and $\beta_o = 0.3$, as we might expect since the calculated β values for "rolling branch" collisions with the soft particle model are usually between the two β_o values used in the hard sphere simulations (see Walton and Braun, 1986a. The large differences in calculated hard-sphere stresses ($\approx$50%) for the two choices of β (*i.e.*, 0 and 0.3) implies that stresses at high solids packings are more sensitive than previously thought to the details of the tangential coupling during collisions. Thus, at high packings it is important to correctly model the effects of the true interaction forces. The algorithm implementing the hard-sphere model collision operator is designed so that it can easily incorporate a non-constant β for the rolling solution; one, for example, which depends on the effective

angle of incidence. This dependence could be an analytic expression or an interpolation table based on more exact collision calculations. Such an addition would only marginally decrease the computational efficiency of the hard-sphere model.

25.7 MICROSTRUCTURE AND STRESS DIFFERENCES

Recent simulations of rapid shearing flows of highly inelastic spheres have exhibited both large first normal stress differences and the formation of clusters of particles (Hopkins and Louge, 1989; Walton et al, 1991) The formation of such clusters is evidently an inherent feature of assemblies of inelastic particles even though no attractive potential is included in the interaction models (Goldhirsch, 1991; Savage, 1992; Babic, 1991). Recent simulations of Zanetti and Goldhirsch indicate that any isolated system of initially uniformly distributed, inelastic particles, with a uniform distribution of velocities will eventually exhibit large variations in the spatial distribution of mass (*i.e.*, large clusters will form as the system 'cools' via collisional energy losses).

Figure 25.10 shows the particles in two identical 'slices' from a calculation of steady shearing flow of inelastic, smooth spheres, with periodic boundaries on all sided. On average, a uniform shear is imposed by moving the image particles in the cell above the primary calculational cell to the right, and those in the image cell below the primary one to the left at constant speed. Each frame shown represents 1/5 of the total calculation space, which contains 4096 particles. The coefficient of restitution in these simulations was 0.01. The particles were initially nearly uniformly distributed throughout the

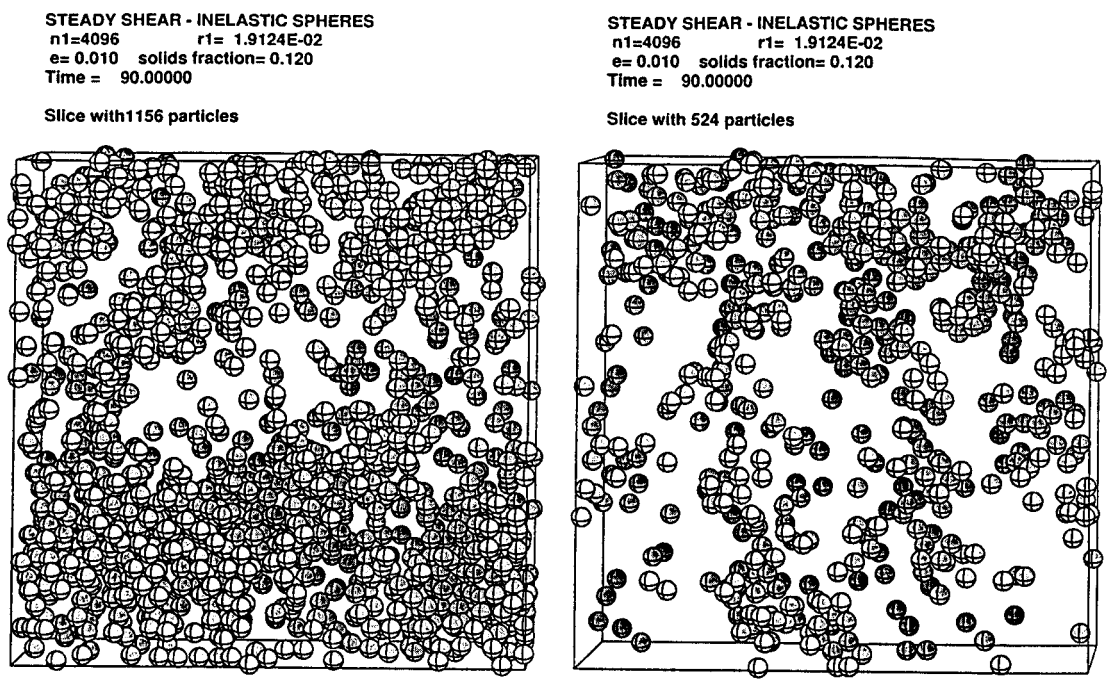

FIGURE 25-10 *Simulation of steady shearing flow of 4096 highly inelastic, e = 0.01, spheres.Two identical size slices, each showing 1/5 of the total volume of the primary calculational cell. after a shear strain of 90. Periodic boundaries on all sides. Note large variation in the distribution of particles.*

cell. The configuration shown is after a total shear deformation of 90 (*i.e.*, distance of 90 cell widths at the time of the image shown). Clearly there are large variations in the density distribution in the calculational cell. The 'cluster' size in this case is on the same order as the calculational cell size -- indicating that the simulation will be of little assistance in determining if there is a 'natural' maximum cluster size that forms in these shearing flows.

Larger sample size simulations have been used in studying cluster formation and growth (Goldhirsch, 1991) and further numerical study of such phenomena will require systems with on the order of 10^6 particles, like the models of Hoover et al. (1990).

25.8 SUMMARY

Discrete particle simulations are providing insight into mechanics that affect the flow behavior of granular solids. Good quantitative agreement has been achieved with chute flow measurements and with theories when the same assumptions are made in the models and the theories. Similar good agreement has been obtained with annular shear cell measurements of shear stress (Walton, 1990)

New phenomena, such as the clusters that were recently "discovered" in low-density simulations (Goldhirsch, 1991, Hopkins and Louge, 1991 and Walton *et al*, 1991) are now the focus of new theoretical studies (Babic, 1991, Savage, 1992, Goldhirsch (& Zanetti) , 1991). Other phenomena, such as large first normal stress differences in steady shearing flows are now generally accepted, and have been incorporated into kinetic theory models for granular materials (Richman and Chou, 1989).

In simulations of systems of interacting particles the physics that distinguishes one material from another is contained in the interaction parameters assumed. Thus, it is important to include a sufficiently realistic model of the "true" interactions if we want the simulated bulk behavior to follow the "true" bulk behavior of the material. Eliminating such details as interparticle friction (and thus all particle rotation) may produce models that are simple and straight forward to evaluate; however, leaving out such important effects may produce a "model material" that bears little resemblance to any real granular material.

A particularly useful feature of discrete particle numerical simulations like the ones described here is that sensitivity studies can be performed in a straight forward manner to determine how individual features of interparticle interactions affect the bulk behavior of the assembly. For example, to see if friction and particle rotations, are important to include, one need merely simulate the flow configuration of interest with, and without, friction in the interparticle interaction.

Based on our present knowledge, it is not possible to make a blanket statement about what effect friction has on the stresses, even in flows as simple as steady rectilinear shear flow. The addition of friction effects can either decrease or increase stresses, depending on the solids concentration and the magnitude of the friction coefficient. This is but one example showing that even dry granular flows are more complex than originally envisioned and that microstructural analyses can provide insight into their behavior.

Dry granular flows remain an important subset of two-phase particulate flow behavior. It is important that we understand the behavior of

the particulate phase as well as the fluid phase. Discrete particle simulations are aiding in that understanding.

25.9 FUTURE WORK

With the advent of massively parallel computers and improved software, we are seeing significant improvements in our ability to simulate the complex phenomena in particulate flows. For example, Hoover *et al*, (1990) describe million-atom molecular dynamics simulations. Such algorithms and parallel processors could also be applied to macroscopic particle simulations. Kim and Fuentes (1992) describe new boundary integral algorithms applicable to suspensions and Ladd and Frenkel (1990) are developing new lattice-Boltzman methods for suspensions. As massively parallel computers become more widely available we can expect to see even more rapid proliferation of new algorithms to take advantage of them, and a corresponding significant improvement in our ability to simulate these complex systems. Direct simulation of flows of engineering interest will soon be possible and future design calculations may well utilize discrete particle flow simulations as routinely as today's fluid flow designers utilize finite element flow codes.

ACKNOWLEDGMENTS

This work was partially supported through the US Department of Energy Office of Fossil Energy, Advanced Research and Technology Development, Solids Transport Program and is funded through the Pittsburgh Energy Technology Center. The DYNA2D calculations and elastic/plastic collision analysis is from unpublished work of Deborah Hagen, conducted during a summer internship at Lawrence Livermore National Laboratory in 1983. The quasistatic calculations and analyses are from previously unpublished work of Julius Brandies in 1984. The author appreciates being able to utilize their work. The original hard-sphere molecular-dynamics code, used with the collision operator described here, was supplied by Tony Ladd. Carlos Caronera provided programming assistance and much of the soft sphere work was done in collaboration with Robert Braun. Work performed under the auspices of the U.S. Department of Energy by Lawrence Livermore National Laboratory under Contract W-7405-Eng-48.

REFERENCES

Ahn, H. and C.E. Brennen, "Channel flows of granular materials and their rheological implications," in *Particulate Two-Phase Flow* (M.C. Roco, ed.) Chapter 7, Butterworth-Heinemann, Boston, (1992).

Alder, B.J. and T. Wainwright, "Studies in Molecular Dynamics, I. General Method," *J. Chem. Phys* **31**, 459 (1959).

Allen, M.P. and D.J. Tildesley, *Computer Simulation of Liquids*, Clarendon Press, Oxford, (1987).

Babic, M. "Particle clustering: an instability of rapid granular flows," in Proceedings. U.S.-Japan Seminar, *Micromechanics of Granular Materials*, Potsdam, NY, Aug 5-9, (1991)

Bagnold, R.A., "Experiments on a gravity-free dispersion of large solid particles in a Newtonian fluid under shear," *Proc. R. Soc. Lond.*,**A225**, 49-63 (1954).

Batchelor, G.K., *J. Fluid Mech.*, **41**,545-570 (1970).

Berne, B.J. "Molecular dynamic of the rough sphere fluid II, Kinetic models of partially sticky sphere, structured spheres, and rough screwballs," *J. Chem. Phys.*, **66**, 2821-30 (1977); also *J. Chem Phys.*, **66**(7) 1745-1754 (1977).

Brach, R.M. "Rigid Body Collisions," *J. Appl. Mech.* (1988).

Brady, J.F. "Stokesian dynamics simulation of particulate flows," in *Particulate Two-Phase Flow* (M.C. Roco, ed.) Chapter 26, Butterworth-Heinemann, Boston, (1992).

Campbell, C.S., "Rapid Granular Flows," *Ann. Rev. Fluid Mech.*, **22**, 57-92,(1990).

Campbell, C.S. and C.E. Brennen "Computer Simulation of Granular Shear Flows," *J. Fluid Mech.*, **151**, 167-188 (1985).

Chapman, S. and T.G. Cowling, *The Mathematical Theory of Non-Uniform Gases*, 2nd ed., Cambridge Univ. Press.(1952, 1970).

Ciccotti, G. and W.G. Hoover, *Molecular Dymnamics Simulations of Statistical-Mechanical Systems*, North-Holland, Amsterdam (1987).

Ciccotti, G., P. Frenkel, and I.R. McDonald, *Simulation of Liquids and Solids*, North-Holland, Amsterdam (1987).

Cundall, P.A., "Rational Design of Tunnel Supports: A Computer Model for Rock Mass Behavior Using Interactive Graphics for the Input and Output of "geometrical Data," Tech. Rept. MRD US Army Corps of Eng., Univ of Minnesota, Rept. Sept. (1974).

Cundall, P.A., and O.D.L Strack, "A discrete numerical model for granular assemblies," *Geotechnique*, **29**, 47-65 (1979); also: *The distinct element method as a tool for research in granular media, Part I.*, Univ. Minn. Rpt. to Nat. Sci. Found. Grant ENG 76-20711 (1979).

Drake, T.G. and R. Shreve "High Speed Motion Pictures of Nearly Steady Uniform, Two-dimensional, Inertial Flows of Granular Material," *J. Rheology*, **30**(5) 981-993 (1986).

Drake, T.G. *Experimental flows of granular materials*, PhD dissertation, UCLA (1988).

Drake, T.G., and O.R. Walton "Comparison of Experimental and Simulated Grain Flows" (in preparation, 1992)

Evans, D.J., "Nonsymmetric Pressure Tensor in Polyatomic Fluids," *J. Stat. Phys.* **20**(5), p547 (1979) .

Frankel, N.A. and A. Acrivos, *Chem. Eng. Sci.*, **22**, 847-853 (1967).

Frisch, U., B. Hasslacher, and Y. Pomeau, *Phys. Rev. Lett.*, **56**, 1505 (1986).

Garwin, R.L., "Kinematics of an Ultraelastic Rough Ball," *Am. J. Phys.*, **37**(1) 88-92 (1969).

Goldhirsch, I., "Clustering Instabilities in Granular Gases," in proceedings *DOE/NSF Workshop on Flow of Particulates and Fluids*, Oct 22-24 1991. S.I. Planski, W.C Peters and M.C. Roco, eds., Nat. Tech., Info. Serv., Springfield, VA, (1991).

Goldsmith, W., *Impact*, E. Arnold Pub., London. (1960).

Goddard, J.D., *J. Non-Newtonian Fluid Mech.*, **142**, 269-287 (1984).

Halquist,J., "DYNA2D--An Explicit Finite Element and Finite Difference Code for Axisymmetric and Plane Strain Calculations," Lawrence Livermore Nat. Lab. Rept. UCRL-52429 (1978).

Halquist,J., "NIKE2D: An Implicit Finite Deformation, finite Element Code for Analyzing the Static and Dynamic Response of Two-Dimensional Solids," Lawrence Livermore Nat. Lab. Rept. UCRL-52678 (1979).

Hawkins, G.W., "Simulation of Granular Flow," in *Mechanics of Granular Materials, New Models and Constitutive Relations*, J.T. Jenkins and M. Satake, eds., Elsevier, 305-312 (1983).

Hertz, H., *J. Math (Crelles's J.)*, **92**, (1881); see also; Timoshenko, S.P. and J.N. Goodier, *Theorgy of Elasticity*, 3rd ed., McGraw-Hill, NY, (1970).

Higuera, F.J. S. Succi and R. Benzi, *Europhys. Lett.*, **9**, 345 (1989).

Hockney, R.W. and J.W. Eastwood, *Computer simulation using particles*, McGraw Hill, NY (1981).

Hoover, Wm. G., *Computational Statistical Mechanics*, Elsevier.Sci. (1991).

Hoover, Wm. G., A.J. DeGroot, C.G. Hoover, I.F. Stowers, T. Kawai, and B.L. Holian, "Large-Scale Elastic Plastic Indentation Simulations via Nonequilibrium Molecular Dynamics," *Phys. Rev. Lett.*,**42** (10) 5844 (1990)

Hopkins, M.A., and H.H. Shen, "A Monte Carlo Simulation of Simple Shear Flow of Granular Materials," in *Micromechanics of Granular Materials*, M. Satake and J.T. Jenkins, eds., Elsevier Sci. Pub. (1988)

Hopkins, M.A., and M.Y. Louge, *Phys. Fluids, A*, **3**(1) p47-57 (1991).

Hunt, K.H. and F.R.E. Crossley, "Coefficients of Restitution Interpreted as Damping in Vibroimpact," *J.Appl. Mech.*,pp440-445, June (1975).

Irving, J.H. and J.G. Kirkwood, *J. Chem. Phys.* **18**(6), 817 (1950).

Johnson, K.L., "Classical vs. Numerical Methods of Elastic Contact Stress Analysis," in *Contact Stress Analysis*, A.D. Roberts and J.E. Muttershead, eds., Institute of Physics, UK Short Mtg Series No. 25, p1-14 (1990).

Johnson, K.L., *Contact Mechanics*, Cambridge Univ. Press, (1985).

Kim, S. and Y.O. Fuentes, "Numerical simulation of suspension flow on high performance computers," in *Particulate Two-Phase Flow* (M.C. Roco, ed.) Chapter 27, Butterworth-Heinemann, Boston, (1992).

Ladd, A.J.C., "Lattice-Boltzman Simulations of Solid-Fluid Processes," to be published, (1992).

Ladd, A.J.C., "Hydrodynamic interactions in a suspension of spherical particles," *J. Chem. Phys.*, **88**, 5051 (1988).

Ladd, A.J.C., "Hydrodynamic transport coefficients of random dispersions of hard spheres," *J. Chem. Phys.*. **93**, 3484 (1990).

Ladd, A.J.C., "Dissipative and fluctuating hydrodynamic interactions between suspended solid particles," in Proc. NATO Adv. Study Institute, *Computer Simulations in Material Science*, M. Meyer and V. Pontikis, eds. (Kluwer Publishers, Dordrecht) (1991).

Ladd, A.J.C. and D. Frenkel, "Dissipative hydrodynamic interactions via lattice-gas cellular automata," *Phys. Fluids*, **A2**, 1921 (1990).

Landau, L.D. and E.M. Lifshitz, *Fluid Mechanics*, Pergamon Press, London (1959).

Leighton, D. and I. Rampall, "Measurement of the shear induced microstructure of concentrated suspensions of non-colloidal spheres," in *Particulate Two-Phase Flow* (M.C. Roco, ed.) Chapter 6, Butterworth-Heinemann, Boston, (1992).

Lun, C.K.K. and S.B. Savage, "A Simple Kinetic Theory for Granular Flow of Rough, Inelastic, Spherical Particles," *J. Appl. Mech.* (1987).

Maw, N., J.R. Barber and J.N. Fawcett "The Oblique Impact of Elastic Spheres," *Wear*, **38** (1) 101-114 (1976).

Maw, N., J.R. Barber and J.N. Fawcett (1981) "The role of Elastic Tangential Compliance in Oblique Impacts,"*Trans ASME, J. Lub. Tech.*, **20**, 327-344.

McNamara, G. and G. Zanetti, *Phys. Rev. Lett.*, **61** 2332 (1988).

McNamara, G. and B.J. Alder, to be published (1992).

Mindlin, R.D. and H. Deresiewicz, *J. Appli. Mech (Trans. ASME)* **20**,327 (1953).

Mindlin, R.D., *J. Appl. Mech (Trans. ASME)* **16**, 259 (1949).

Mullier, M., U. Tuzun and O.R. Walton, "A single-particle friction cell for measuring contact frictional properties of granular materials," *Powder Technology*, **65**, 61-74, 1991.

Nakagawa, N. "Kinetic Theoretical Approach for Rapidly Deforming Disk Assembly," in *Micromechanics of Granular Materials*, M. Satake and J.T. Jenkins, eds., Elsevier Sci. Pub. (1988); see also: N. Nakagawa, PhD. Thesis, Cornell University (1987).

Nunan, K.C. and J.B. Keller, "Effective Viscosity of a Periodic Suspension," *J. Fluid Mech.*, **142**, 269-287 (1984).

Oden,J.T. and J.A.C. Martins, "Models and Computational Methods for Dynamic Friction Phenomena," Proceedings: Fenomech III in: *Computer Methods in Applied Mechanics and Engineering*, North Holland, Amsterdam (1984).

Patrakis, E., R. Dobry, T.T. Ng and L. Liu, *A Study of the Behavior and Micromechanical Modeling of Granular Solids*, Civil Eng. Rept., Rensselaer Polytech. Inst., Troy, NY, USAF Contract No. AFOSR-89-0350.(1991).

Prosperetti, A. and A.S. Sangani, "Numerical simulation of the motion of particles at large Reynolds numbers," in *Particulate Two-Phase Flow* (M.C. Roco, ed.) Chapter 28, Butterworth-Heinemann, Boston, (1992).

Richman, M.W., and C.S. Chou, *J.Rheology*, **33** (8), 1292 (1989).

Savage, S.B. "Instability of an unbounded uniform granular shear flow," *J. Fluid Mech.* (in press 1992).

Sears, J.E., "On the Longitudinal Impact of Metal Rods with Rounded Ends," *Trans. Camb. Phil. Soc.*, **21**, 49, (1908).

Timoshenko, S.P. and J.N. Goodier, *Theory of Elasticity*, 3rd ed. McGraw-Hill, NY (1970).

Thornton, C., and C.W. Randall, "Application of Theoretical Contact Mechanics to Solid Particle System Simulations," in *Micromechanics of Granular Materials*, M. Satake and J.T. Jenkins, eds., Elsevier Sci. Pub. (1988).

van den Brule, B.H.A.A., and R.J.J. Jongschaap, "Modeling of Concentrated Suspensions," *J. Stat. Phys.*, **62**(5/6) 1225-1237 (1991).

Veseley, F.S. *Mol. Phys.*, **41**, 5, 959-1015 (1980).

Walton, O.R. and R.L. Braun, "Viscosity and Temperature Calculations for Assemblies of Inelastic Frictional Disks," *J. Rheology*, **30**(5), 949-980 (1986a).

Walton, O.R., R.L. Braun, R.G. Mallon and D.M. Cervelli, "Particle-Dynamics Calculations of Gravity Flow of Inelastic, Frictional Spheres," in *Micromechanics of Granular Materials*, M. Satake and J.T. Jenkins, eds., Elsevier Sci. Pub. (1988)

Walton, O.R., R.L. Braun, "Stress Calculations for Assemblies of Inelastic Spheres in Uniform Shear," *Acta Mechanica*, **63**, 73-86 (1986b)

Walton, O.R., K.A. Hagen, and J.M. Cooper, "Interparticulate Force Models for Computational Simulation of Granular Solids Flow," presented at 16th International Congress of Theoretical and Applied Mechanics, Lyngby, Denmark 19-25, Aug (1984a).

Walton, O.R., J. Brandeis, and J.M. Cooper, "Modeling of Inelastic, Frictional, Contact Forces in Flwoing Granular Assemblies," *Abstracts*, 21st Annual Mtg. Soc of Eng. Sci., Blacksburg, VA, p257, (1984).

Walton, O.R., "Computer Simulation of Rapidly Flowing Granular Solids," *Science on Form*, S. Ishizaka, ed., KTK Sci. Pub., Tokyo, p175-189 (1990).

Walton, O.R., "Numerical Simulation of Inclined Chute Flows of Monodisperse, Inelastic Frictional Spheres," *Mech. of Mat.* (in press, 1992).

Walton, O.R., H. Kim, and A.D. Rosato, "Microstructure and Stress Differences in Shearing Flows," *Mechanics Computing in 1990's and Beyond*, H. Adeli and R.L. Sierakowski, eds., ASCE, NY, Vol 2, p1249-1253 (1991).

Particulate Two-Phase Flow

Edited by

M.C. Roco

National Science Foundation and
University of Kentucky

With 50 contributing authors

Butterworth–Heinemann

Boston London Oxford Singapore Sydney Toronto Wellington

Library of Congress Cataloging-in-Publication Data

Particulate two-phase flow / edited by M.C. Roco, with 50 contributing authors.
p. cm. — (Butterworth-Heinemann series in chemical engineering)
Includes bibliographical references and index.
ISBN 0-7506-9275-8 (alk. paper)
1. Two-phase flow. 2. Particles. I. Roco, M. C. II. Series.
TA357.5.M84P37 1992
620.1'064—dc20 92-33076
CIP

British Library Cataloguing-in-Publication Data
A catalogue record for this book is available from the British Library.

Butterworth–Heinemann
80 Montvale Avenue
Stoneham, MA 02180

10 9 8 7 6 5 4 3 2 1

Printed in the United States of America